HYDROLOGICAL PROCESSES
Hydrol. Process. **16**, 873–890 (2002)
DOI: 10.1002/hyp.366

Stable isotopes in river ice: identifying primary over-winter streamflow signals and their hydrological significance

J. J. Gibson[1]* and T. D. Prowse[2]
[1] *Department of Earth Sciences, University of Waterloo, Waterloo, Ont. N2L 3G1, Canada*
[2] *National Water Research Institute, 11 Innovation Blvd., Saskatoon, Sask. S7N 3H5, Canada*

Abstract:

The process of isotopic fractionation during freezing in the riverine environment is discussed with reference to a multi-year isotope sampling survey conducted in the Liard–Mackenzie River Basins, northwestern Canada. Systematic isotopic patterns are evident in cores of congelation ice (black ice) obtained from rivers and from numerous tributaries that are recognized as primary streamflow signals but with isotope offsets close to the equilibrium ice–water fractionation. The results, including comparisons with the isotopic composition of fall and spring streamflow measured directly in water samples, suggest that isotopic shifts during ice-on occur due to gradual changes in the fraction of flow derived from groundwater, surface water and precipitation sources during the fall to winter recession. Low flow isotopic signatures during ice-on suggest a predominantly groundwater-fed regime during late winter, whereas low flow isotopic signatures during ice-off reflect a mixed groundwater-, surface water- and precipitation-fed regime during late fall. Copyright © 2002 John Wiley & Sons, Ltd.

KEY WORDS river ice; streamflow; stable isotopes; oxygen-18; deuterium; hydrograph separation; fractionation

INTRODUCTION

River, lake and sea ice covers are a valuable archive of changing climate, and specifically hydroclimatic conditions occurring through the winter (Ferrick and Prowse, 2000). Methods applied to extract hydroclimatic information from ice cores have included sediment, geochemical and isotopic characteristics of ice. Depth and spatial distributions of the stable isotopes of water (δ^{18}O and δ^{2}H) in ice cores are particularly important in that they can be used to decipher modes and rates of ice formation, ice type and water sources (MacDonald *et al*., 1995; Eichen, 1998; Bowser and Gat, 1995; Ferrick *et al*., 1998; Gibson and Prowse, 1998, 1999). From the perspective of watershed studies, isotopic analysis of river ice offers unique opportunities for reconstructing the isotopic composition of streamflow and may assist in tracing extreme events or gradual changes in over-winter hydrological processes (Gibson and Prowse, 1999).

The isotopic signature of river ice depends on several factors: (i) the primary isotopic composition of water from which it forms, (ii) the variable offset produced by isotopic fractionation during freezing which is controlled by ice-growth velocity and boundary layer conditions (Ferrick *et al*., 1998), (iii) the presence/absence of reservoir effects in the liquid phase which may produce extreme isotopic changes in ice due to fractional crystallization (e.g. Gibson and Prowse, 1999) and (iv) post-freeze-up complexities. Such complexities in the ice record, both physical and isotopic, may arise from modification of the river ice cover by mechanical disruption during freeze-up, depositional changes related to snow loading, slushing,

* Correspondence to: J. J. Gibson, Isotope Hydrology Section, International Atomic Energy Agency, Wagramer Strasse 5, PO Box 100, Vienna, Austria. E-mail: j.gibson@iaea.org

Received 14 August 2000
Accepted 28 December 2000

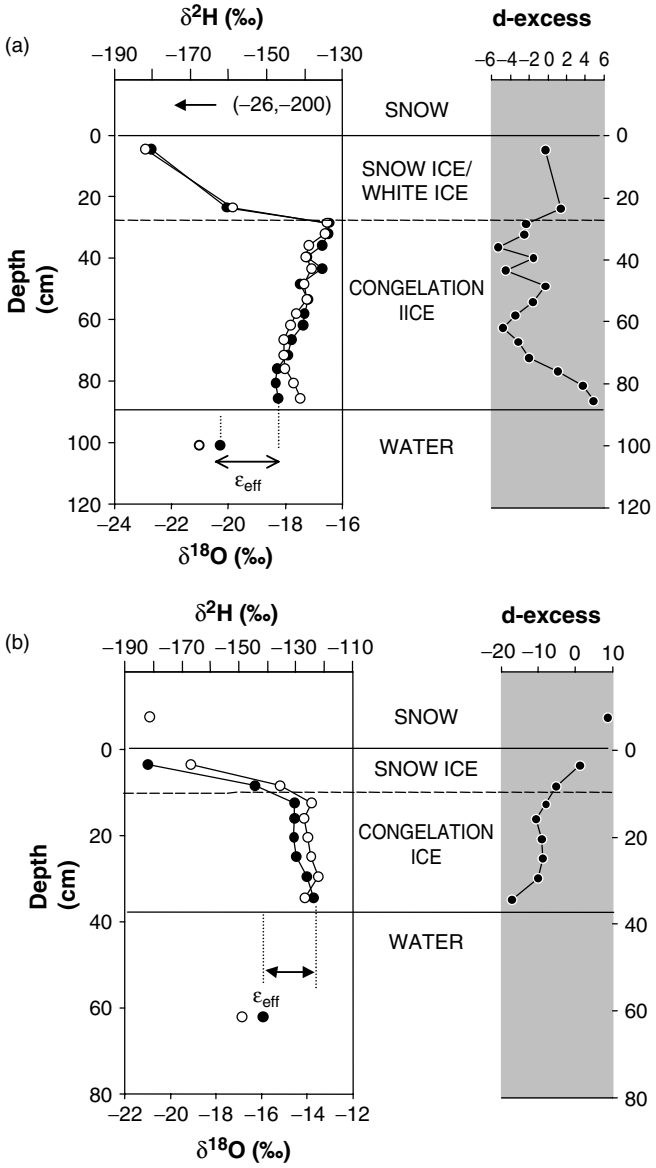

Figure 1. Vertical isotopic distribution and d-excess in ice cores collected in the Liard River Basin, March 1998: (a) Blackstone River near the mouth; (b) Poplar River near the mouth. Closed and open circles denote $\delta^{18}O$ and $\delta^{2}H$, respectively and ε_{eff} denotes the observed ice–water isotopic separation. d-Excess, defined as $d = \delta^{2}H - 8\delta^{18}O$, is plotted as an evaporation index or index of departure from the MWL, where $d \sim 10$ reflects a precipitation–groundwater dominated source plotting close to the MWL. Progressively lower d-excess, in the range of $10 > d > -30$, reflects increasing contributions from surface water sources, especially lakes. Note that the Blackstone River, a wetland-dominated tributary, becomes depleted in the heavy isotopic species, with an associated increase in d-excess over time/depth, whereas the Poplar River, a lake affected tributary, becomes progressively enriched in the heavy isotopic species and tends toward lower d-excess values

frazil accumulation, anchor ice deposition and mechanical or thermal erosion. Such factors must be taken into consideration when an ice core is selected for use as a proxy for the isotopic composition of streamflow.

This study applies isotopes in river ice to gain insight into winter streamflow processes in remote areas of the Liard Basin, a catchment of 277 000 km^2 situated in northwestern Canada and draining to the Arctic

Ocean via the Mackenzie River. From field observations it is demonstrated that the isotopic signature of streamflow is systematically preserved in congelation ice (black ice, see Adams, 1981)—clear, coarse grained often columnar ice growing in still reaches—that is obtained from uncomplicated river ice covers, avoiding conditions noted in (iv) above to ensure that ice is formed *in situ* under conditions that favour slow ice growth, and turbulent, non-restricted mixing of the source water under ice.

Vertical distributions of stable isotopes in such uncomplicated river ice covers (Figure 1) are generally characterized by the presence of an upper layer of white, polycrystalline ice which is depleted in the heavy isotopes due to incorporation of snow, and an underlying zone of congelation ice that may preserve, from top to bottom, a frozen archive of the temporal isotopic changes that have occurred in streamflow over the course of the winter. Less systematic isotopic distributions are expected in ice cores that are not specifically selected to avoid the complications noted above (e.g. Ferrick *et al*., 1998; Bowser and Gat, 1995).

One important condition for this type of analysis is that the ice–water fractionation is known or can be well constrained. In the present setting, the isotopic composition of new basal ice is shown to be systematically offset from the formation water during late winter, although by slightly less than the equilibrium ice–water isotopic fractionation. As shown, changes in isotopic composition during the ice-on period (i.e. duration of season that ice cover is present) are found to be reasonable and consistent with isotopic compositions measured in water samples collected before and after the ice-on period, which suggests that the basic method is valid. To provide a basis for discussion, the following sections include a review of the relevant theory followed by an overview of isotopic characteristics of streamflow and source waters in the study area.

THEORY

Ice–water fractionation

Isotopic fractionation during freezing is known to occur due to preferential incorporation of the rare, heavy isotopic species of water ($^{1}H^{1}H^{18}O$ and $^{1}H^{2}H^{16}O$) into the ice phase relative to the common light species ($^{1}H^{1}H^{16}O$) (Moser and Stichler, 1980). This process is not reversible however. Due to low mobility of molecules in the ice phase, melting is generally a non-fractionating process. For thermodynamic equilibrium between phases, the freezing ice–water fractionation can be expressed by a reaction rate constant also known as the equilibrium isotopic fractionation α^* given by

$$\alpha^* = \frac{R_{\text{ice}}}{R_{\text{water}}} \tag{1}$$

such that $\alpha^* = 1$ for zero fractionation and $\alpha^* > 1$ for natural freezing conditions, where R is $^{18}O/^{16}O$ or $^{2}H/^{1}H$. Equilibrium fractionation is also expressed using the isotopic separation factor ε^* defined by

$$\varepsilon^* = 1000(\alpha^* - 1) = \delta_{\text{ice}} - \delta_{\text{water}} \tag{2a}$$

$$\varepsilon^* \approx 1000 \ln \alpha^* \tag{2b}$$

with units of per mil (‰) analogous to δ values which express isotopic ratios as deviations in per mil from Vienna-SMOW (Standard Mean Ocean Water) where

$$\delta_{\text{SAMPLE}} = 1000[(R_{\text{SAMPLE}}/R_{\text{V-SMOW}}) - 1] \tag{3}$$

Experimental estimates of ε^* near 0 °C at natural freezing rates (<2 mm/h) in freshwater systems range from about 2·8 to 3·1‰ for oxygen (Suzuoki and Kimura, 1973; O'Neil, 1968) and 17·0 to 20·6‰ for hydrogen (Kuhn and Thürkauf, 1958; Arnason, 1969; see also Moser and Stichler, 1980). Recent work by Ferrick *et al*. (1998) may indicate that some of the observed experimental variability in ε^* arises due to slight differences in experimental conditions, i.e. slight dissimilarity in crystal growth rate and flow conditions

adjacent to the interface which may inhibit attainment of thermodynamic equilibrium between ice and water. Lower equilibrium separations are also generally associated with elevated salinity as observed for sea ice (MacDonald *et al*., 1995). Ferrick *et al*. (1998) present a model for the effective freezing fractionation based on a 1D advection–diffusion model in which isotopic exchange is controlled by flow-induced (turbulent) mixing of the water and on diffusive resistance to mixing in a thin (0 to 4-mm thick) boundary layer at the ice–water interface. The model is mechanistically similar to the Craig and Gordon model of the evaporation process (see Craig and Gordon, 1965; Gat, 1996) except that diffusive resistance acts to reduce the effective ice–water fractionation rather than increasing it as observed for the evaporation process. Ferrick *et al*. (1998) define an effective fractionation factor α_{eff} where

$$\alpha_{\text{eff}} = \frac{\alpha^*}{\alpha^* + (1 - \alpha^*) \exp\left[\dfrac{-z\nu}{D_i}\right]} \tag{4}$$

and where z is the boundary layer thickness (mm), ν is the velocity of ice growth (cm/day) and D_i is the self-diffusion coefficient for $^1H_2{}^{18}O$ or $^1H^2H^{16}O$ (cm^2/day). The effective or total isotopic fractionation α_{eff} is the product of the equilibrium α^* and kinetic fractionation factors α_K as

$$\alpha_{\text{eff}} = \alpha^* \alpha_K \tag{5}$$

and the corresponding kinetic isotopic separation factor ε_K can be defined in an analogous way by substituting Equation (2b) into Equation (5) and $\varepsilon_K \approx 1000 \ln \alpha_K$ as

$$\varepsilon_{\text{eff}} = \varepsilon^* + \varepsilon_K \tag{6}$$

Note that $\varepsilon_{\text{eff}} \to \varepsilon^*$ for slow ice growth and thin diffusional boundary layers. According to the model proposed by Ferrick *et al*. (1998), which assumes pure diffusion in the boundary layer (Figure 2), ε_K is postulated

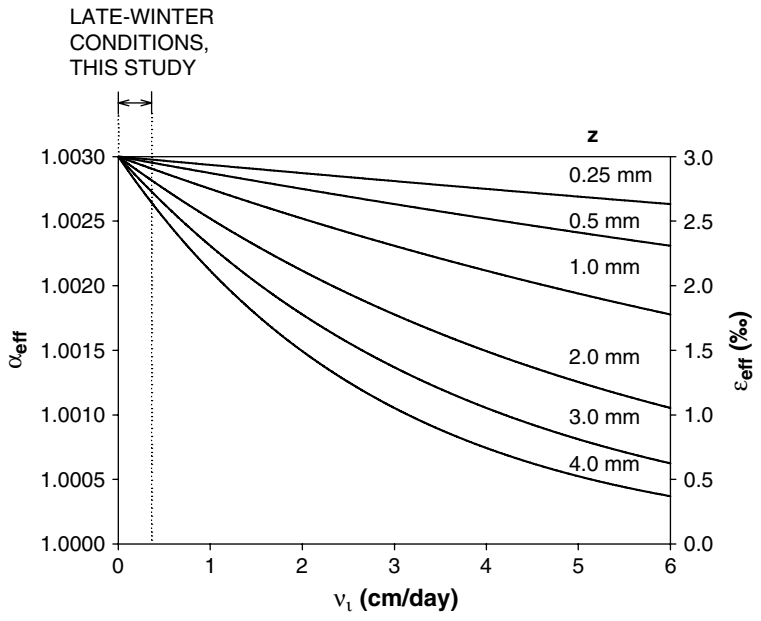

Figure 2. Plot of ice growth velocity ν_i versus effective ice–water separation ε_{eff} for a range of boundary layer thicknesses z. The plot assumes ε^* for oxygen of 3·0‰ (created using the formula of Ferrick *et al*., 1998). Note the range of values anticipated for late winter conditions in this study

to range from values of 0‰ for oxygen in the case of very slow ice growth (1–3 mm/day) to as much as −2·5‰ in oxygen for the case of a well-developed boundary layer (4 mm thick) and very rapid ice growth (6 cm/day). The predicted isotopic separations have been shown to be in agreement with results from laboratory experiments for flow rates of about 0·3 m/s (Ferrick, personal communication). The range of anticipated isotopic separation values for late winter in the Liard–Mackenzie Basin is shown in Figure 2.

Reservoir isotope effects

Along margins of river channels, or in shallow areas, ice may grow near to or in contact with the underlying bed or anchor ice, thereby affecting the local flow regime. As such it may be possible in some areas for sub-ice conduits to become wholly or partially disconnected from the main river channel. In shallow channels and lakes, this effect may be extreme. From the perspective of isotopic reconstructions, source water signals may become convoluted if ice cores are extracted from disconnected areas.

When ice forms from a wholly disconnected (closed) reservoir (Figure 3a), the isotopic composition of ice and water will maintain the offset defined by ε_{eff} but will progressively deplete with time according to a Rayleigh-type fractional crystallization process. In this situation, the instantaneous isotopic composition of new ice (δ_{R}) is given by

$$\delta_{\text{R}} = (\delta_0 + 1000)\, f^{(\alpha^* - 1)} - 1000 \tag{7}$$

where $f = V/V_0$ is the fraction of water remaining, V and V_0 are the volume of the liquid at the time of ice formation and the initial volume, respectively, and δ_0 is the isotopic composition of the original liquid (Michel, 1986). Closed-system freezing leads to progressive heavy isotope depletion in both ice and residual water which can overwhelm primary sourcewater signals and lead to extreme isotopic gradients in ice as compared to non-restricted open system conditions (Figure 3c). In the case where flow is only partially disconnected from the reservoir, a more likely occurrence in riverine environments, gradients may be more subtle (Figure 3b) but may still overwhelm primary sourcewater signals.

Other effects

Effective isotopic separation ε_{eff} is expected to vary with depth throughout the ice cover due to freezing rate effects as predicted by the diffusion models (see Figure 3d). It is important to note that ice growth rates are generally less than 0·6 cm/day on average over the course of the winter in the study area, which is the likely reason why near equilibrium values of ε_{eff} are commonly observed (Gibson and Prowse, 1999).

Complex processes such as frazil accumulation, snow incorporation, freeze–melt–freeze cycles, flooding and other complications can lead to significant changes in isotopic composition of an ice cover and as such can be used to trace aspects of ice cover history (Ferrick *et al.*, this issue). In general, cores with complex features may be less reliable for reconstructing the isotopic composition of streamflow.

ISOTOPIC COMPOSITION OF STREAMFLOW AND ITS SOURCES

Previous studies in the lower Liard Basin near Ft. Simpson (Gibson *et al.*, 1993a,b; Gibson and Prowse, 1998, 1999) and ongoing hydrological process studies within the Mackenzie GEWEX Study (Rouse, 2000) have involved characterization of the isotopic composition of streamflow and its primary sources, i.e. snow, rain, groundwater and surface water including wetlands and lakes. On a plot of δ^{18}O versus δ^{2}H (Figure 4), streamflow and its sources are shown to be labelled by their isotopic composition, and define two distinct linear trends in δ^{18}O–δ^{2}H space. Precipitation, including snow and rain, falls close to the meteoric water line (MWL) defined by $\delta^{2}\text{H} = 8\delta^{18}\text{O} + 10$ (Craig, 1961). Variations in the isotopic composition of rain and snow, snow being depleted in the heavy isotopes with respect to rain, are mainly related to temperature-dependent effects during condensation of atmospheric moisture and air mass history. Meteoric waters that have undergone evaporation, including lakes and wetlands (surface waters, Figure 4) display systematic

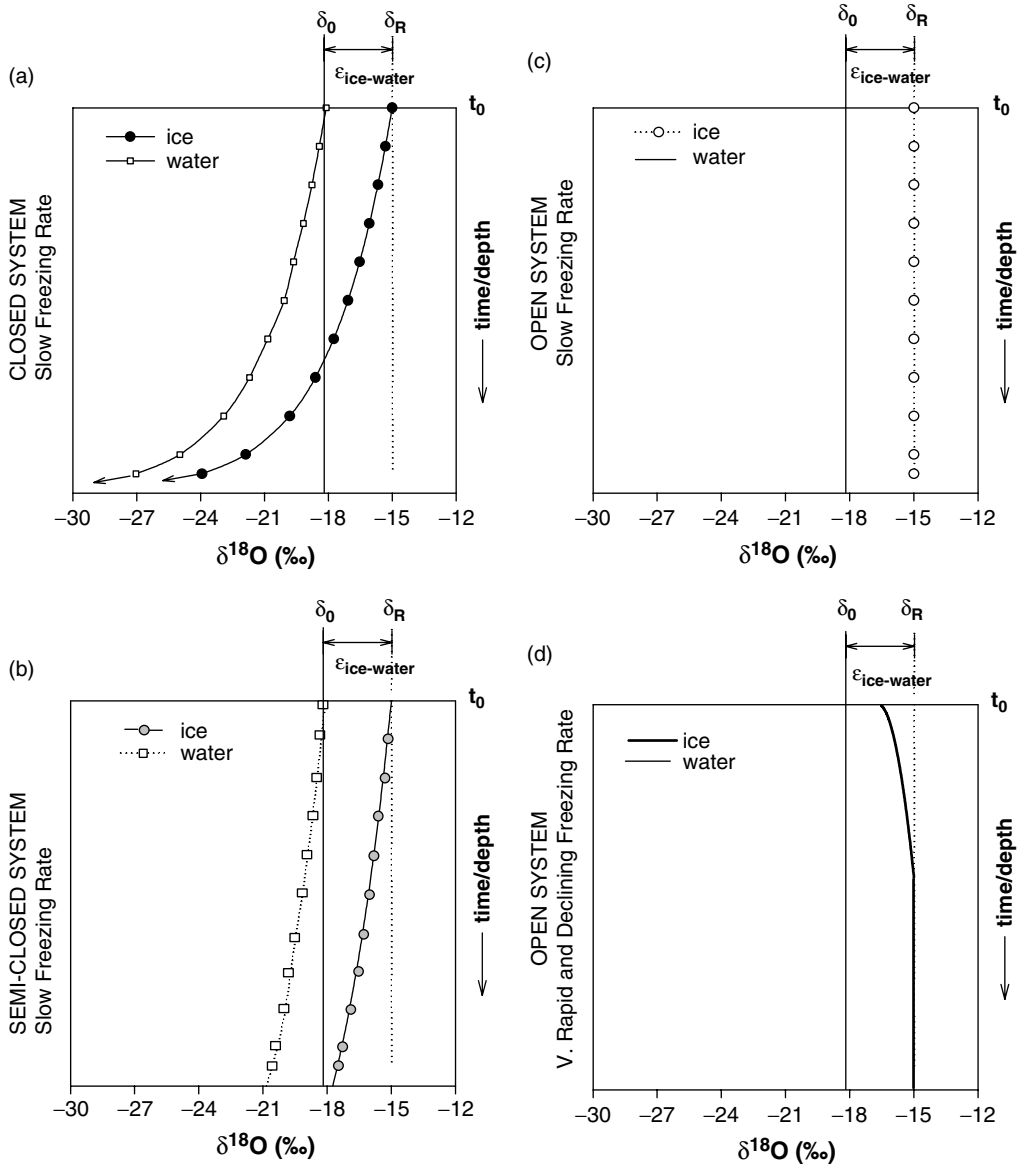

Figure 3. Plots of $\delta^{18}O$ versus depth of ice illustrating the reservoir and freezing rate effects. (a) Closed system with slow freezing, (b) semi-closed system with slow freezing, (c) open system with slow freezing rate, (d) open system with very rapid and declining freezing rate. Note that δ_0 is the initial isotopic composition of the liquid and δ_R is the initial isotopic composition of ice. The trends presented in (a)–(c) assume constant isotopic separation between ice and water $\varepsilon_{ice-water}$

enrichment in ^{18}O and ^{2}H, resulting in divergence along a local evaporation line (LEL; Figure 4) defined by $\delta^2H = 4{\cdot}9\delta^{18}O - 64$ ($r^2 = 0{\cdot}95$, $n = 26$). The slope and intercept of the LEL in Figure 4, and also peak enrichment levels determined from 1997–1999 ice-off sampling, are in close agreement with values obtained from sampling surveys in 1989–1990 ($\delta^2H = 5{\cdot}0\delta^{18}O - 64$; $r^2 = 0{\cdot}95$, $n = 57$), suggesting very stable enrichment conditions. A useful approximation of $\delta^{18}O$ and δ^2H in mean annual precipitation is obtained from the intersection of the MWL and LEL, in principle representing the annual weighted input

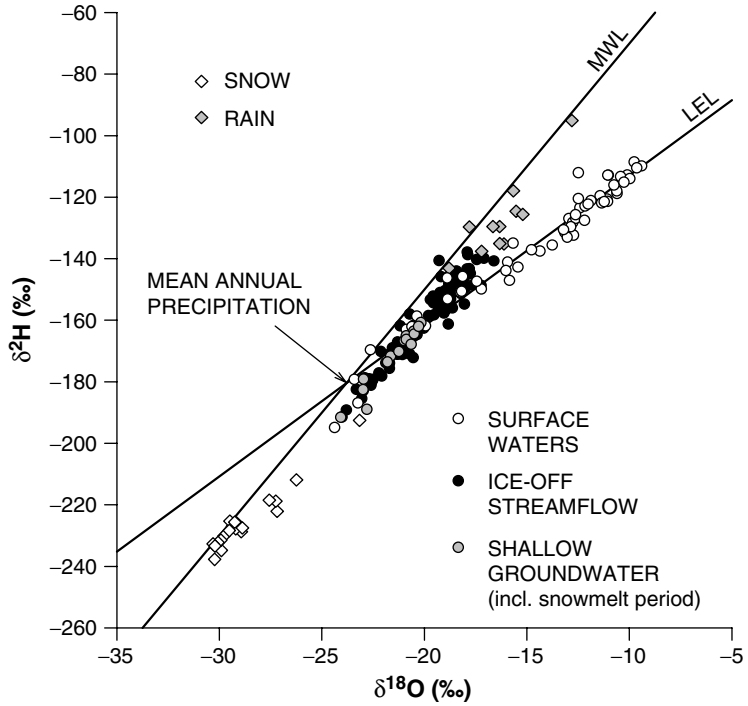

Figure 4. Plot of $\delta^{18}O$ versus $\delta^{2}H$ illustrating the isotopic composition of snow, rain, surface waters, mean annual precipitation, groundwater and ice-off streamflow for the Ft. Simpson area. Note that local surface waters lie along an LEL while rain, snow, groundwater and streamflow lie close to the MWL of Craig (1961). Streamflow during snowmelt is depleted relative to summer/fall streamflow, producing a general trend towards, more enriched values during the course of the ice-off period. See text for discussion

to surface waters. Several rain samples plot below the MWL, reflecting evaporation from raindrops during descent through unsaturated air. Apart from the snowmelt period when the effects of recharge of snowmelt are pronounced, groundwaters tend to be fairly uniform and plot slightly below the MWL, reflecting some evaporative enrichment of these reservoirs. Shallow groundwater trends closely parallel the MWL primarily as a result of the effect of snowmelt mixing with pre-existing groundwater.

Snowmelt is also the dominant control on the ice-off variations seen in the isotopic composition of streamflow. From the time of peak snowmelt, streamflow in Ft. Simpson area tributaries tends to enrich parallel to the MWL as snowmelt contributions wane and mixtures of post-melt groundwater, rain and surface water begin to dominate. One important characteristic of ice-off streamflow in the area is that streams display different levels of evaporative isotopic enrichment in the summer, reflecting water balance conditions in contributing areas within each basin (see Gibson *et al.*, 1993a). In an analogous way to groundwater, snowmelt mixing sets the general streamflow trend in $\delta^{18}O$–$\delta^{2}H$ space (Figure 4). Evidence of isotopic changes in streamflow during the transition from late fall to late winter, as discerned from ice archives, are discussed later on in this paper.

STUDY AREA AND METHODS

Ice coring and water sampling in the Liard–Mackenzie Basin were conducted in consecutive years during the late winter (March) of 1997, 1998 and 1999. Activities in the first year focused on collection of ice cores at the regional scale, mainly from the Liard River along its lower reaches and from selected tributaries (see Figure 1 in Gibson and Prowse, 1999). Activities in the second and third years targeted tributaries to

the Liard River near Ft. Simpson (Figure 5), for which isotope records during April through October were being collected as part of a hydrograph separation analysis under way within the Mackenzie GEWEX Study (Rouse, 2000). The mean maximum ice thickness in rivers in the area ranges from 75 to 150 cm, with mean freeze-up dates close to 15 November and mean ice-free dates close to 15 April (Prowse, 1990) A total of 14 congelation ice cores were extracted during 1997, seven during 1998 and eight during 1999. Ice cores were sampled in late March and represented near maximum ice thicknesses in smooth ice reaches. Ice thickness was generally greater but more variable in mechanically disrupted areas.

Coring sites were selected close to hydrometric gauging stations so that discharge estimates were also available. Where possible, cores were extracted from smooth ice reaches near the centre of the main river channel. If uncomplicated ice cores dominated by congelation ice were not obtained, then other cores were collected in adjacent or nearby areas. Coring locations were determined precisely using a GPS (Global Positioning System).

Depth-integrated snow samples were obtained before coring at each site using a standard snow tube. Snow was then sealed in thick-walled HDPE (high-density polyethylene) bags. Prior to coring, the snow cover was carefully removed from a 1-m × 1-m area of the ice using a snow shovel and brush. Ice cores were then extracted using a gas-powered 70·8-mm diameter ice corer, capable of extracting continuous cores of up to 75 cm. An extension was available so that cores up to 150-cm thick could be collected. Once extracted, cores

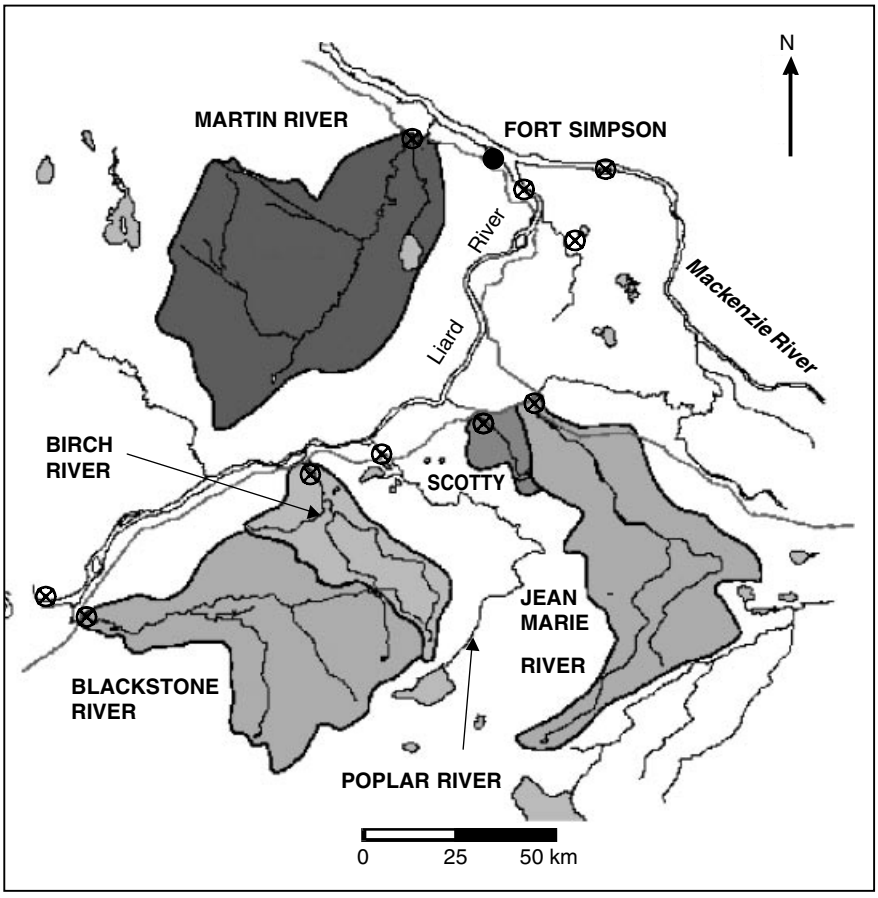

Figure 5. Map of the Ft. Simpson area, Northwest Territories, Canada showing coring locations for 1998 and 1999 in the lower Liard River near the mouth. Watershed areas of wetland streams from Figure 8 are included

were extruded from the core barrel onto a dry polyethylene tarp. Cores were then photographed, logged for ice type and thickness, and 5 to 10-cm subsamples were sawed apart using a mitre box and transferred to thick-walled HDPE bags. At base camp, ice and snow samples were allowed to melt entirely at room temperature and then transferred to 125-ml HDPE bottles. Water samples were collected at mid-depth between the base of river ice and bed using a drop sampler, and were placed in 1-L HDPE bottles. During the 1998 survey, selected samples were also obtained in a similar way from water that filled the borehole after coring.

Isotope samples were returned to the Environmental Isotope Laboratory, University of Waterloo for analysis of oxygen and hydrogen stable isotopes using standard methods. $\delta^{18}O$ and $\delta^{2}H$ results cited herein are reported relative to V-SMOW and normalized to both V-SMOW (0‰, 0‰) and SLAP (Standard Light Antarctic Precipitation; −55·5‰ and −428‰, respectively) (see Coplen, 1996). Analytical uncertainty is estimated to be ±0·1‰ for $\delta^{18}O$ and ±2‰ for $\delta^{2}H$.

RESULTS AND DISCUSSION

Ice–water fractionation

The isotopic composition of basal ice (<5 cm thick) and mid-depth water was compared for 29 ice cores comprised mainly of *in situ* congelation ice (Tables I and II). Of the 29 cores, nine were excluded due to non-ideal conditions, i.e. parts of the core contained layers of slush and/or liquid water, or the core was frozen to the bed, or in one case the core stratigraphy was unusual due to proximity to a waterfall. Many additional cores were judged in the field to be complex and unsuitable for reconstructing the isotopic composition of streamflow and so were discarded or were returned to the laboratory but not analysed. From direct comparisons of basal congelation ice and mid-depth water in the 20 ideal locations, for ice thicknesses ranging from 36 to 93 cm, the effective ice–water isotopic separation ε_{eff} is found to be $2{\cdot}84 \pm 0{\cdot}34$‰ for oxygen and $17{\cdot}9 \pm 3{\cdot}9$‰ for hydrogen. These values are consistent with ε_{eff} predicted by the model of Ferrick *et al*. (1998) for slow ice growth (between 0·6 and 1 cm/day), assuming a boundary layer thickness of 1 mm and ε^{*} for oxygen and hydrogen of 3·00‰ and 20·0‰, respectively. Such ice growth rates and boundary layer thicknesses are reasonable for late winter conditions in the study area. Note that the non-ideal cores were found to have highly variable ice–water separations and are not included in the calculation of the mean.

Mean values of ε_{eff} estimated from 1997 samples alone, which reflected sampling primarily in locations along the main channel of the Liard and Mackenzie River, were $2{\cdot}94 \pm 0{\cdot}33$‰ for oxygen and $19{\cdot}5 \pm 1{\cdot}6$‰ for hydrogen as reported by Gibson and Prowse (1999). Slightly higher values and reduced variability observed for this group of samples may reflect consistently lower ice growth rates and thinner boundary layers (i.e. more turbulent flow) in the main rivers than in the tributaries.

One anomalous sample collected in 1999 (LIARD) was found to have an unusually low ε_{eff} for hydrogen of 9‰, although it was an uncomplicated ice core comprised mainly of congelation ice and did not exhibit any unusual characteristics. Analytical or reporting errors could not be ruled out as there was insufficient sample volume to permit a repeat analysis. If this sample is removed then the mean value of ε_{eff} for hydrogen becomes $18{\cdot}3 \pm 3{\cdot}4$‰.

For late winter ice–water pairs, plots of $\delta^{18}O_{WATER}$ vs. $\delta^{18}O_{ICE}$ and $\delta^{2}H_{WATER}$ vs. $\delta^{2}H_{ICE}$ illustrate the systematic nature of the ice–water isotopic separation (Figure 6). Best-fit lines lie subparallel and in close proximity to the theoretical equilibrium separation trends, and indicate no pronounced relationship between δ values and ε_{eff} (i.e. isotope content does not affect the ice–water separation), which is expected from theoretical considerations. Overall, the behaviour of oxygen isotopes during freezing appears to be more regular or predictable than for hydrogen, although both isotopes are required to distinguish evaporative enrichment effects.

Direct estimates of ε_{eff} based on ice–water pairs provide a useful field-based measure of the magnitude of late winter isotopic fractionation. Although not directly characterized in this study, it has been shown in laboratory experiments that ε_{eff} is generally reduced by up to 0·6‰ in oxygen (∼4‰ in hydrogen) in the

Table I. Summary of congelation ice–water $\delta^{18}O$ and physical characteristics, 1997–1999

Site	Type	Year	Ice and snow properties						Sub-ice water		Basal ice (‰)	ε_{eff} (‰)
			Total ice thickness (cm)	Snow depth (cm)	Snow + ice depth (cm)	Sub-ice water depth (cm)	Hydrostatic water level (cm)	Complications	Mid-depth (‰)	In-hole (‰)		
FNAL	main	97	42	43	85	328	5	–	−20·97	–	−17·72	3·25
L1	main	97	76	31	107	354	0	–	−21·71	–	−18·56	3·15
L2	main	97	54	22	76	316	0	–	−21·69	–	−18·73	2·96
LAB	main	97	50	56	106	370	5	–	−21·62	–	−19·03	2·60
LAP	main	97	93	35	128	167	−2	–	−21·59	–	−18·83	2·76
LASNE	main	97	66	22	88	444	–	–	−21·22	–	−18·53	2·69
LASNW	main	97	65	20	85	455	–	–	−21·49	–	−18·49	3·00
M1	main	97	75	13	88	780	–	–	−17·46	–	−14·65	2·81
SCOTTY	trib	97	53	45	98	32	11	Sl	−21·29	–	−17·74	3·55*
FNAM	trib	97	73	27	100	10	–	Sl	−20·55	–	−16·96	3·59*
MUS	trib	97	48	30	78	25	–	–	−21·18	–	−18·47	2·71
SN	trib	97	50	13	63	133	–	–	−22·81	–	−20·08	2·73
POPLAR	trib	97	50	42	92	8	−31	–	−16·66	–	−14·14	2·52
PET	trib	97	68	43	111	80	1	–	−12·74	–	−15·57	2·83
LIARD	main	98	56	30	86	228	−1	–	−21·42	−21·55	−18·63	2·79
POPLAR	trib	98	48	20	68	26	−20	Sl	−15·65	−15·78	−13·72	1·93*
JEAN-MARIE 1	trib	98	64	16	80	36	−5	Sl	−22·72	−25·78	−17·21	5·51*
JEAN-MARIE 2	trib	98	77	26	103	173	3	–	−20·3	−20·53	−17·17	3·13
BLACKSTONE	trib	98	87	2	89	29	−6	Sl	−24·84	−25·55	−18·28	6·56*
SCOTTY	trib	98	42	27	69	23	−20	–	−19·81	−19·86	−16·94	2·87
BIRCH R.	trib	98	34	36	70	0	−14	Fb	−20·62	−16·41	−16·74	3·88
LIARD	main	99	66	37	103	236	1	–	−21·31	–	−19·03	2·28
JEAN-MARIE 1	trib	99	59	38	97	191	3	–	−19·55	–	−17·34	2·21
BLACKSTONE	trib	99	55	32	87	6	−31	–	−20·87	–	−18·08	2·79
SCOTTY	trib	99	51	10	61	11	−44	Sl	−24·32	–	−17·31	7·01*
BIRCH R.	trib	99	51	39	90	0	−10	Fb	−20·82	–	−17·71	3·11
MR01	trib	99	36	44	80	34	−11	–	−16·64	–	−14·01	2·63
TR01	trib	99	71	10	81	22	−3	Wf	−22·51	–	−14·74	7·77*
TL01	lake	99	76	26	102	84	3	–	−16·88	–	−14·17	2·71
Mean			60	29	89	159	−6					2·84
1 Std			14	13	15	185	12					0·34

Main, Liard River; trib, tributary; Sl, slush/liquid water layers; Fb, frozen to near bottom; Wf, waterfall nearby; *not included in calculation of mean, std.

Table II. Summary of congelation ice–water δ^2H and physical characteristics, 1997–1999

Site	Type	Year	Ice and snow properties						Sub-ice water		Basal ice (‰)	ε_{eff} (‰)
			Total ice thickness (cm)	Snow depth (cm)	Snow + ice depth (cm)	Sub-ice water depth (cm)	Hydrostatic water level (cm)	Complications	Mid-depth (‰)	In-hole (‰)		
FNAL	main	97	42	43	85	328	5	–	−162·4	–	−143·5	18·9
L1	main	97	76	31	107	354	0	–	−170·6	–	−152·3	18·3
L2	main	97	54	22	76	316	0	–	−169·7	–	−148·9	20·8
LAB	main	97	50	56	106	370	5	–	−170·5	–	−151·7	18·8
LAP	main	97	93	35	128	167	−2	–	−170·1	–	−153·1	17·3
LASNE	main	97	66	22	88	444	–	–	−171·1	–	−149·0	22·1
LASNW	main	97	65	20	85	455	–	–	−168·8	–	−151·9	16·9
M1	main	97	75	13	88	780	–	–	−145·4	–	−125·2	20·2
SCOTTY	trib	97	53	45	98	32	11	Sl	−168·7	–	−147·8	20·9*
FNAM	trib	97	73	27	100	10	–	Sl	−159·1	–	−137·2	21·9*
MUS	trib	97	48	30	78	25	–	–	−167·2	–	−147·9	19·3
SN	trib	97	50	13	63	133	–	–	−182·1	–	−160·4	19·6
POPLAR	trib	97	50	42	92	8	−31	–	−147·0	–	−128·2	18·8
PET	trib	97	68	43	111	80	1	–	−138·2	–	−121·8	18·6
LIARD	main	98	56	30	86	228	−1	–	−165·9	−165·6	−152·2	13·7
POPLAR	trib	98	48	20	68	26	−20	Sl	−138·4	−134·7	−126·9	11·5*
JEAN-MARIE 1	trib	98	64	16	80	36	−5	Sl	−176·1	−193·5	−137·0	39·1*
JEAN-MARIE 2	trib	98	77	26	103	173	3	–	−161·0	−155·3	−142·0	19·0
BLACKSTONE	trib	98	87	2	89	29	−6	Sl	−189·7	−192·9	−141·3	48·4*
SCOTTY	trib	98	42	27	69	23	−20	–	−155·9	−157·7	−141·2	14·7
BIRCH R.	trib	98	34	36	70	0	−14	Fb	−164·5	−127·3	−136·7	27·8
LIARD	main	99	66	37	103	236	1	–	−163·4	–	−154·4	9·0
JEAN-MARIE 1	trib	99	59	38	97	191	3	–	−155·9	–	−143·7	12·2
BLACKSTONE	trib	99	55	32	87	6	−31	–	−162·4	–	−149·0	13·4
SCOTTY	trib	99	51	10	61	11	−44	Sl	−188·4	–	−142·6	45·8*
BIRCH R.	trib	99	51	39	90	0	−10	Fb	−162·7	–	−140·3	22·4
MR01	trib	99	36	44	80	34	−11	–	−143·5	–	−128·1	15·4
TR01	trib	99	71	10	81	22	−3	Wf	−178·9	–	−124·6	54·3*
TL01	lake	99	76	26	102	84	3	–	−138·5	–	−121·5	17·0
Mean			60	29	89	159	−6					17·9
1 Std			14	13	15	185	12					3·9

Main, Liard River; trib, Liard tributary; Sl, slush/liquid water layers; Fb, frozen to near bottom; Wf, waterfall nearby; *not included in calculation of mean, std.

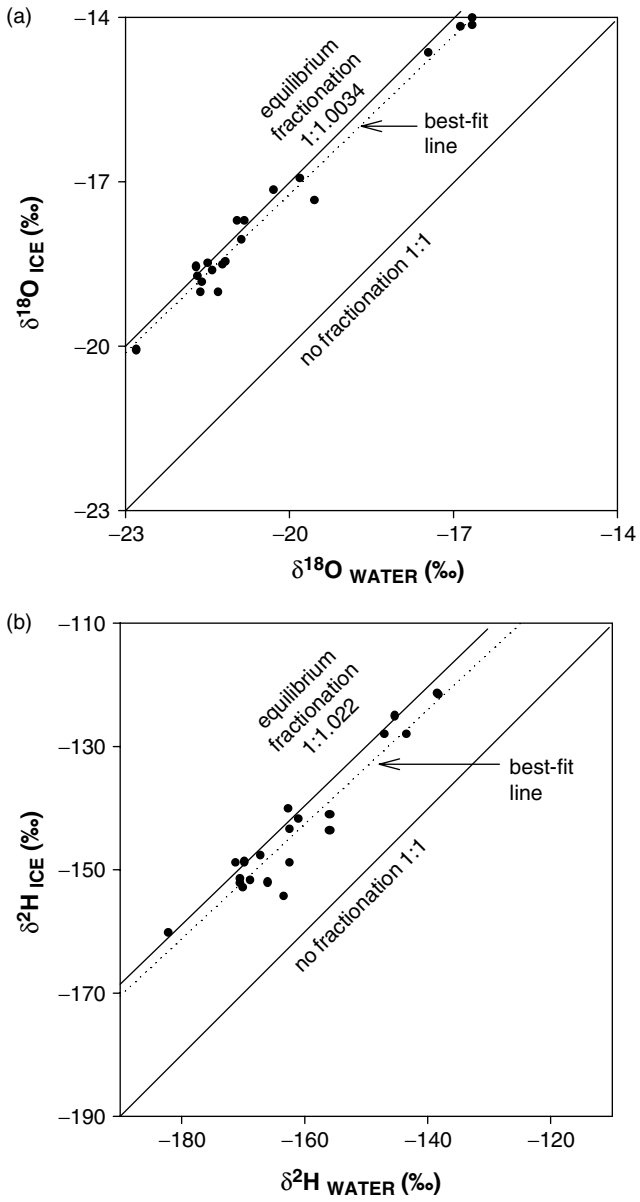

Figure 6. Plots of ice–water isotope pairs as sampled in late winter: (a) $\delta^{18}O_{WATER}$ vs. $\delta^{18}O_{ICE}$ and (b) $\delta^{2}H_{WATER}$ vs. $\delta^{2}H_{ICE}$ illustrating the systematic nature of the ice–water isotopic separation. Best-fit lines lie subparallel and in close proximity to the theoretical equilibrium separation trends, and indicate no pronounced relationship between δ values and ε_{eff}

uppermost 20 cm or so of ice due to the freezing rate effect (Figure 3b; see also Ferrick *et al.*, this issue). Such effects are relatively small compared to streamflow shifts inferred in the smaller tributaries. As for the main river channels, near-constant vertical profiles of $\delta^{18}O$ and $\delta^{2}H$ were obtained in the Mackenzie River ice core (see Figure 5 in Gibson and Prowse, 1999) which is most simply explained by near-constant ε_{eff} and near-constant isotopic composition of streamflow, the latter of which is expected considering that water is derived from a large reservoir, Great Slave Lake. This indirect evidence suggests that freezing rate effects

may be subdued in the present setting, at least in the large rivers. In any case, this influence is likely to be significant during the first month or less of ice growth.

As discussed previously, the effect of freezing rate on isotopic fractionation is expected to vary with depth of ice. Lack of significant trends between ε_{eff} and ice thickness (Figure 7a) and ice + snow thickness (not shown) also lends support for the assertion that this effect may be minor, at least in the range of observed ice thickness (42–93 cm) and snow depth (2–44 cm) recorded in late March.

One notable observation is that the effective isotopic separation ε_{eff} is found to be insensitive to water depth for ideal cores, but highly sensitive to water depth for non-ideal cores below a threshold water depth of about 40 cm (Figure 7b). Evidently, restricted water depths can have a significant impact on the magnitude of the ice–water separation and on the presence of slush/water layers, which may in part be attributed to reservoir effects produced by restricted circulation of liquid water. In some cores, isotopic fractionation in such cores was up to 2·5 times the equilibrium values, and is likely due to reservoir effects.

Water samples collected from boreholes in 1998 were found in some cases to be isotopically similar to those obtained at mid-depth. In other cases, samples were found to be depleted in $\delta^{18}O$ and $\delta^{2}H$, potentially reflecting snowmelt bypass, i.e. water with a high content of snowmelt in a centimetre-thick layer immediately below the ice cover (e.g. Bergmann and Welch, 1985). Sensitivity of the ice–water separation to very shallow water depths (Figure 7b) and presence of heavy-isotope depleted water under or within the ice cover may in some cases simply be the result of restricted circulation effects, as expected for a closed or semi-closed system (Figures 3a and b).

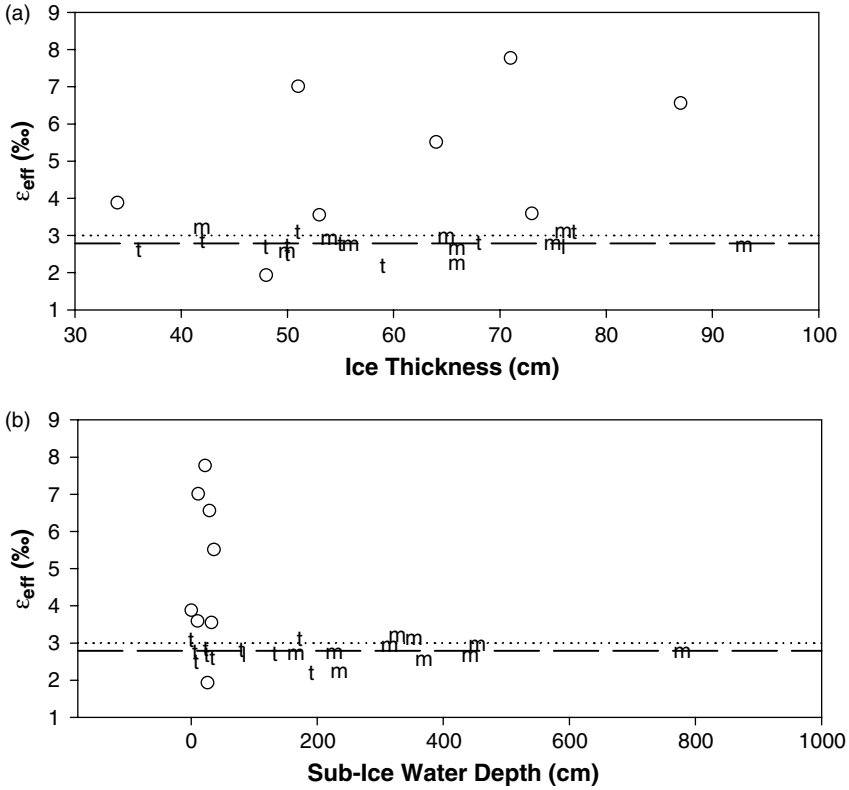

Figure 7. Plots of ε_{eff} vs. ice thickness and sub-ice water depth based on oxygen-18. Note that ideal congelation ice cores are obtained from tributaries (t) and the main river channel of the Liard or Mackenzie Rivers (m). Non-ideal ice cores are shown as open circles. See text for discussion

Vertical ice profiles

Examples of vertical profiles of $\delta^{18}O$ and $\delta^{2}H$ in ice cores obtained in the surveys are shown in Figure 1. Additional profiles from 1997 including lakes were presented in Gibson and Prowse (1999). Cores were identified that became more depleted in $\delta^{18}O$ with depth (e.g. Figure 1a) and others that became more enriched in $\delta^{18}O$ with depth (Figure 1b). All streams gauged by the Water Survey of Canada were of the type that became more depleted in $\delta^{18}O$. Streams that tended to become more enriched with depth/time displayed corresponding shifts to lower *d*-excess, which is consistent with increases in contributions of water from surface reservoirs (likely lakes) that had previously undergone significant evaporative enrichment. The tributaries that became enriched in the heavy isotopic species over the course of the winter also tended to be lake-affected, i.e. contained abundant lakes. One mechanism that may account for ice-on enrichment in streamflow is snow loading on lake ice, a process that can displace water from lakes with outlets that remain open throughout the winter. Snow loading can be a significant contributor to streamflow, second only to groundwater, and has been shown to account for more than 10% of winter discharge in some subarctic lakes (Adams, 1981). Ice flexing may also contribute to short-term pulses of winter discharge (Adams, 1981), although this does not explain the gradual overwinter shifts in isotopic composition that were observed.

Reconstructed isotopic composition of streamflow

The isotopic composition of streamflow for selected tributaries to the Liard was reconstructed from vertical profiles assuming observed values for the ice–water separation ε_{eff} of $2{\cdot}84 \pm 0{\cdot}34‰$ for oxygen and $18{\cdot}3 \pm 3{\cdot}4‰$ for hydrogen, assuming that ice growth was continuous and proportional to $\sqrt{t}$ according to the model of Prowse (1995). While this is a simple representation and ignores potential variations in ε_{eff} due to freezing rate effects, the results suggest that the approach can be used to determine broad ice-on trends. Time series of isotopic composition of streamflow reconstructed from ice profiles and from ice-off water sampling are shown along with discharge records (Figure 8). Similar trends were observed for ^{2}H (not shown).

Time series plots show consistency between ice-off and ice-on isotopic composition of streamflow in terms of signatures and continuity, which provides support for the use of the simple reconstruction approach adopted herein. The most pronounced anomalies between the water sampling and ice reconstructed records are found in the Blackstone and Birch Rivers in late March, and attributed to reservoir effects due to limited water depth. Importantly, the reconstructed streamflow values serve as a valuable tool for obtaining a winter isotopic record from a single late winter field visit in areas that would otherwise be impractical to sample on a regular basis. Inter-annual isotopic records for cold-region watersheds, as shown in Figure 8, have not been reported widely in the literature.

In general, the seasonal cycle of discharge and isotopic composition in wetland-dominated tributaries is defined by a snowmelt recession which occurs from April to June followed by frequent rainfall events in late summer. Low flow during ice-off occurs in late fall during extended rain-free periods and is typically the most enriched water due to a high content of surface water relative to rain. Isotopic signatures suggest that groundwater remains the dominant overall source. The ice-on period, as reconstructed from ice records, is dominated by the fall-to-winter recession in which discharge diminishes and isotopic signatures become progressively more depleted in the heavy isotopes due to extended reduction in surface water sources (Figure 8). In lake-dominated tributaries the winter period is characterized by slight enrichment in heavy isotopes, presumably due to snow loading effects, although there is a lack of discharge data for lake-affected tributaries to test this hypothesis at the current time. A comparison of isotopic signatures of low flow during ice-on and ice-off for wetland and lake-affected tributaries reveals that the latter type tends to be more enriched in heavy isotopes during both periods (Table III, Figure 9). This attests to the distinct influence of lakes on the hydrological regime of some basins in the area.

$\delta^{18}O$ vs. $\delta^{2}H$ relationships

A plot of $\delta^{18}O$ and $\delta^{2}H$ (Figure 9) depicts the isotopic composition of low flow during both the ice-on and ice-off period. Low flow during ice-off is shown to plot below the MWL and close to but slightly above the

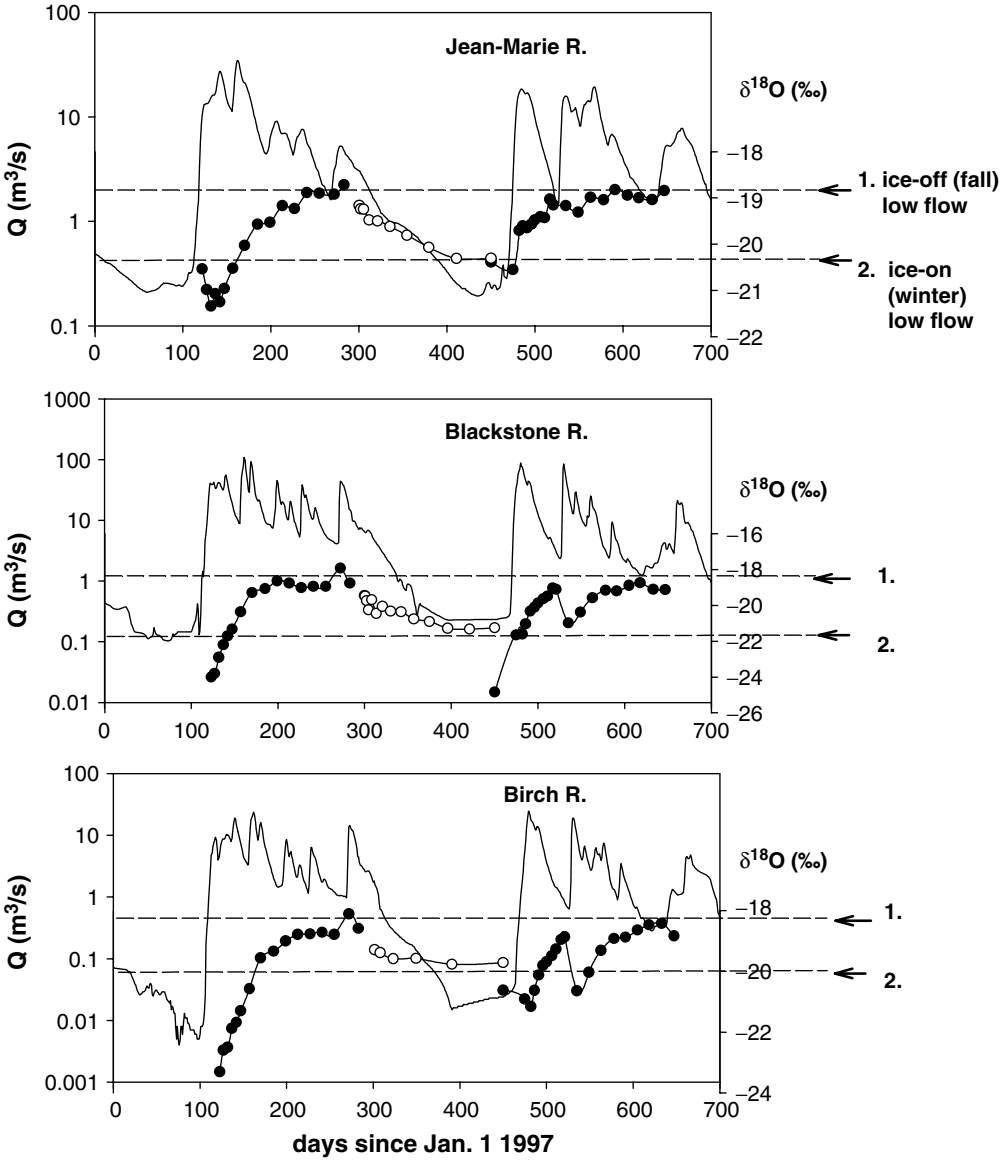

Figure 8. Time series of isotopic composition of streamflow in tributaries to the Liard River. Open circles depict values reconstructed from ice archives and solid circles represent water samples collected during ice-off. Note that no ice core was extracted at Martin River in 1998. Note that average snowpack composition determined in snow surveys was found to be −29·0‰ in $\delta^{18}O$ and −227‰ in $\delta^{2}H$. Average groundwater composition is estimated to be −20·0‰ in $\delta^{18}O$ and −164‰ in $\delta^{2}H$, plotting close to ice-on (winter) low flow values

LEL, reflecting a mixture of groundwater, surface water and rain sources. Ice-on low flow is shown to be enriched in the heavy isotopes in the case of lake-affected streams, and depleted in the heavy isotopes in the case of wetland streams. In contrast to the snowmelt recession, isotopic shifts in the fall-to-winter recession tend to occur along the LEL and in general record a reduction in streamflow contributions from rainfall and a shift in the proportion of groundwater versus surface water sources. A best-fit line drawn through winter low flow values yields a relation similar to the LEL based on sampling of local lakes and wetlands during summer, reflecting the absence of rainfall in streamflow at this time.

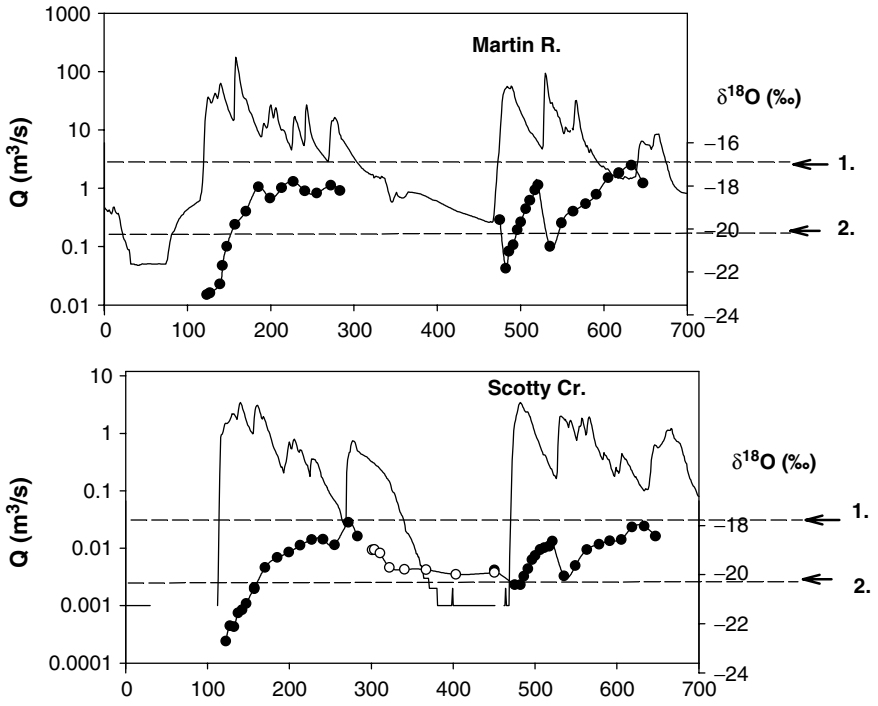

Figure 8. (*Continued*)

Table III. Low flow isotopic signatures for ice-on and ice-off in tributaries to the Liard–Mackenzie Rivers

	Year	Ice-on (winter) low flow		Ice-off (fall) low flow	
		$\delta^{18}O$ (‰)	$\delta^{2}H$(‰)	$\delta^{18}O$ (‰)	$\delta^{2}H$(‰)
Wetland tributaries					
Blackstone R.	98	−21·3	−162	−19·0	−153
	99	−21·0	−168	−18·8	−154
Birch R.	98	−19·7	−156	−18·8	−152
	99	−20·7	−160	−18·4	−151
Jean-Marie R.	98	−20·3	−156	−18·9	−157
	99	−20·3	−163	−19·0	−152
Scotty Cr.	98	−19·9	−161	−18·6	−147
	99	−20·2	−162	−18·0	−146
mean		−20·4	−161	−18·7	−151
Lake-affected tributaries					
Poplar R.	97	−17·1	−148	–	–
Petitot R.	97	−15·7	−141	–	–
Martin R.	98	–	–	−18·3	−147
	99	−17·0	−148	−17·4	−143
Trout R.	99	−17·7	−144	–	–
mean		−16·8	−145	−17·7	−145

It is important to note that the isotopic composition of low flow during the ice-free period is potentially useful for partitioning free-surface evaporation losses from watersheds (Gibson *et al*., 1993a), whereas the isotopic composition of low flow during ice-on contains useful information on the role of lakes and groundwater

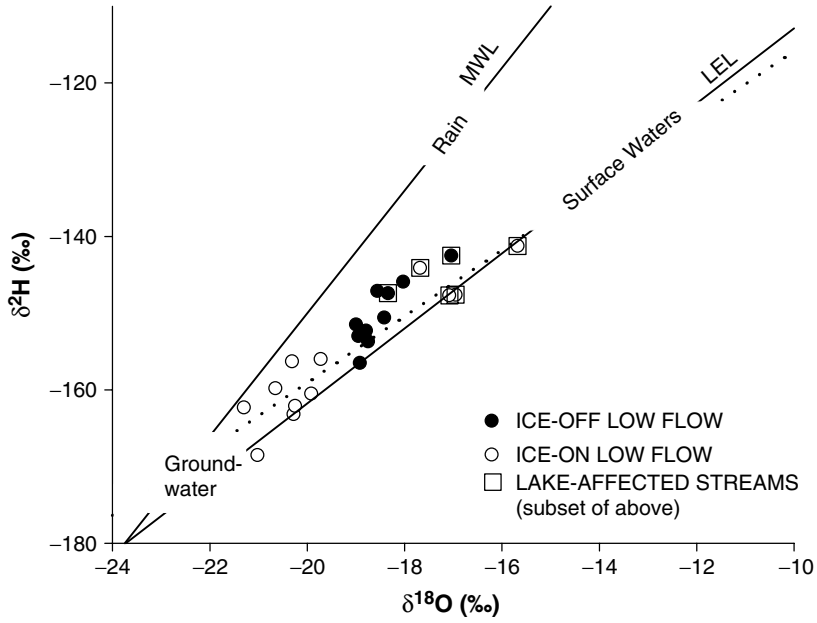

Figure 9. Plot of $\delta^{18}O$ versus $\delta^{2}H$ illustrating the isotopic signature of low flow during ice-off and ice-on. Also shown are the local evaporation line and meteoric water line (LEL and MWL, respectively). Low flow signatures during ice-off are controlled by mixing of groundwater, surface water and rain. Low flow signatures during ice-on lie close to the LEL, reflecting the absence of rainfall. Relative to ice-off signatures, ice-on signatures are enriched for lake-affected tributaries and depleted for wetland tributaries, reflecting proportionate mixing of groundwater and surface water

and their contribution to the winter discharge. Together, water sampling and ice core reconstructions of isotopes in streamflow provide a more complete picture of inter-annual hydrograph response in a cold-region watershed. Although beyond the scope of this paper, isotopes in streamflow may also be applied in the context of hydrograph separation analysis to identify the timing and magnitude of source water contributions (groundwater, surface water, rain and snow) for complete annual cycles, which is expected to be a valuable tool for improving hydrologic models in the area.

CONCLUDING REMARKS

The method used for reconstruction of isotopes in streamflow is found to yield satisfactory results that may be improved by incorporating a more sophisticated representation of the ice–water fractionation process. The principle drawback encountered with the approach was that tributaries may freeze to the bottom in some areas, thus causing the isotopic fractionation process to be complicated or overprinted by reservoir effects. To avoid this problem cores should be taken in areas where water depth is greater than about 50 cm.

One obvious direction for future research is to obtain time series of ice cores and water samples at regular intervals throughout a complete winter to verify the constancy of ε_{eff} and to identify the possible effects of erosion/non-deposition of ice due to mid-winter thawing or development of gaps between ice and underlying water, particularly in small tributaries. This has yet to be carried out due to high cost and logistical difficulties associated with conducting winter field operations in the area.

The observed trends in isotopic composition of streamflow emphasize the need to distinguish between ice-on and ice-off conditions in cold-region watersheds, as baseflow or low flow is strongly influenced by ice cover. Furthermore, isotopes in river ice demonstrate that lake-affected tributaries may be a distinct hydrological regime or subregime that is not well represented by the current Water Survey of Canada monitoring network.

ACKNOWLEDGEMENTS

The Liard ice and snow surveys were carried out by Tom Carter and Cuyler Onclin, NWRI Saskatoon, with the support of the Water Survey of Canada, Fort Simpson. Laboratory isotope analysis was performed by staff of the Environmental Isotope Laboratory, University of Waterloo. This work was funded by research grants from the Canadian GEWEX Study and the National Water Research Institute. This manuscript benefited from the comments of Mike Ferrick and three anonymous reviewers.

REFERENCES

Adams WP. 1981. Snow and ice on lakes. In *Handbook of Snow: Principles, Processes, Management and Use*, Gray DM, Male DH (eds). Pergamon Press: Toronto; 437–474.

Arnason B. 1969. Equilibrium constant for the fractionation of deuterium between ice and water. *Journal of Physical Chemistry* **73**: 3491–3494.

Bergmann MA, Welch HE. 1985. Spring meltwater mixing in small arctic lakes. *Canadian Journal of Fisheries and Aquatic Science* **42**: 1789–1798.

Bowser CJ, Gat JR. 1995. On the process of lake-ice formation. In *Proceedings International Symposium on Isotopes in Water Resources Management*. IAEA-SM-336/44P, International Atomic Energy Agency: Vienna.

Coplen TB. 1996. New guidelines for reporting stable hydrogen, carbon, and oxygen isotope-ratio data. *Geochimica et Cosmochimica Acta* **60**: 3359–3360.

Craig H. 1961. Isotopic variations in meteoric waters. *Science* **133**: 1833–1834.

Craig H, Gordon LI. 1965. Deuterium and oxygen 18 variations in the ocean and marine atmosphere. In *Stable Isotopes in Oceanographic Studies and Paleotemperatures*, Tongiorgi E (ed.). Lab. Geologia Nucleare: Pisa; 9–130.

Eichen H. 1998. Factors determining microstructure, salinity and stable-isotope composition of Antarctic sea ice: deriving modes and rates of ice growth in the Weddell Sea. In *Antarctic Sea Ice: Physical Processes, Interactions and Variability*, Jefferies M (ed.). AGU Ant. Res. Series **74**; 89–122.

Ferrick MG, Prowse TD. 2000. Two communities join forces to study ice-covered rivers and lakes. *EOS* **81**(10): 108.

Ferrick MG, Calkins DJ, Perron NM. 1998. Stable environmental isotopes in lake and river ice cores. In *Ice in Surface Waters*, Shen HT (ed.). Balkema: Rotterdam; 207–214.

Ferrick MG, Calkins DJ, Perron NM, Cragin JH, Kendall C. 2002. Diffusion model validation and interpretation of stable isotopes in river and lake ice. *Hydrological Processes* **16**(4): 851–872.

Gat JR. 1996. Oxygen and hydrogen isotopes in the hydrologic cycle. *Annual Review of Earth and Planetary Science* **24**: 225–262.

Gibson JJ, Prowse TD. 1998. Isotopic characteristics of ice cover in a large northern river basin. In *Ice in Surface Waters*, Shen HT (ed.). Balkema: Rotterdam; 197–205.

Gibson JJ, Prowse TD. 1999. Isotopic characteristics of ice cover in a large northern river basin. *Hydrological Processes* **13**: 2537–2548.

Gibson JJ, Edwards TWD, Bursey GG, Prowse TD. 1993a. Estimating evaporation using stable isotopes: quantitative results and sensitivity analysis for two catchments in northern Canada. *Nordic Hydrology* **24**: 79–94.

Gibson JJ, Edwards TWD, Prowse TD. 1993b. Runoff generation in a high boreal wetland in northern Canada. *Nordic Hydrology* **24**: 213–224.

Kuhn W, Thürkauf M. 1958. Isotopentrennung biem gefrieren von wasser und diffusionskonstanten von D und ^{18}O im eis. *Helvitiva Chimica Acta* **41**: 938–971.

MacDonald RW, Paton DW, Carmack EC, Omstedt A. 1995. The freshwater budget and undersea spreading of Mackenzie River water in the Canadian Beaufort Sea based on salinity and $^{18}O/^{16}O$ measurements in water and ice. *Journal of Geophysical Research* **100**(C1): 895–919.

Michel FA. 1986. Isotope geochemistry of frost-blister ice, North Fork Pass, Yukon, Canada. *Canadian Journal of Earth Science* **23**: 543–549.

Moser H, Stichler W. 1980. In *Handbook of Environmental Isotope Geochemistry*, Vol. 2, Fritz P, Fontes JCh (eds). Elsevier: New York; 141–178.

O'Neill JR. 1968. Hydrogen and oxygen isotope fractionation between ice and water. *Journal of Physical Chemistry* **72**: 3683–3684.

Prowse TD. 1990. Northern hydrology: An overview. In *Northern Hydrology: Canadian Perspectives*, Prowse TD, Ommanney CSL (eds). NHRI Science Report No. 1, National Hydrology Research Institute, Environment Canada: Saskatoon; 1–36.

Prowse TD. 1995. River ice processes. In *River Ice Jams*, Beltaos S (ed.). Water Resources Publications: Highlands Ranch; 29–70.

Rouse WR. 2000. Progress in hydrological research in the Mackenzie GEWEX Study, *Hydrological Processes* **14**: 1667–1685.

Suzuoki T, Kimura T. 1973. D/H and $^{18}O/^{16}O$ fractionation in the ice–water system. *Mass Spectroscopy* **21**: 229–233.

